250 Meter Wire Antenna Deployer Mechanism

Scotty R. Allen*

Abstract

A wire antenna deployer for the Radio Plasma Imager (RPI) instrument on the Imager for Magnetopause-to-Aurora Global Exploration (IMAGE) spacecraft has been developed and qualified for space flight by AEC-Able Engineering Company, Incorporated (ABLE). Performance specifications; design of the deployer mechanism; and lessons learned during the design, manufacturing and testing phases of the program are presented. Unique aspects of this design include a mechanism capable of withstanding sustained high voltages in excess of 6400 VAC, an internal wire tensioning device, and use of stepper motors to provide simultaneous antenna deployment in the spin plane of the spacecraft of 4 deployers at virtually identical rates.

Introduction

Four, 250-meter wire antenna deployers form part of the RPI instrument on the IMAGE spacecraft scheduled to be launched into an elliptical, polar orbit using a Delta II rocket on, 1 January 2000, from Vandenberg Air Force Base. The orbit, measuring 1000km × 7 Earth radii, will carry the spacecraft through the Van Allen radiation belts out to the edges of the magnetosphere. The spacecraft is spin stabilized at 0.052 rad/s (0.5 rpm). The four, 250-meter wire antennas spaced at 90 degrees around the spacecraft perimeter deploy radially outward in the spin plane of the spacecraft, thus forming a pair of crossed dipole antennas. Digitally synthesized radio signal pulses in frequencies between 3 kHz and 3 MHz are transmitted on these radial dipole antennas. These same antennas then act as receivers for the signals reflected from the plasma structure of the Earth's magnetosphere. The scope of this paper is limited to the design, manufacture, test, and lessons learned associated with the antenna deployment mechanisms. Other aspects of the RPI instrument are beyond the scope of this paper.

Many of the lessons learned during the development, manufacturing and test of the wire antenna deployer were qualitative in nature. While laborious and excruciating quantitative technical or analytical detail may be of value to this specific design, the purpose of this paper is to present enough technical detail to understand the operation of the mechanisms and to get a feel for the relative magnitude of those aspects of the mechanism performance that relate to the lessons learned

*AEC-Able Engineering Company, Inc., Goleta, CA

Performance Specifications

The qualification testing demonstrated that the wire deployer met the performance parameters described in Table 1, Wire Deployer Specifications and Performance. The deployment rate of the antenna is determined by software-controlled clock signals sent from the spacecraft computer (CPU) to the stepper motor controller. The mass of the deployer does not include the transceiver electronics. Radiation hardness was not tested; however, components in the stepper motor controller are designed to withstand radiation exposure greater than 100 krad.

Table 1, Wire Deployer Specifications and Performance

Deployed Antenna Length	250 m (820 ft)
Deployment Rate	Programmable 0.7 to 1.5 cm/sec
High Voltage Capability	6400 VAC (6kHz); 2250 VDC
Mass	4.8 kg (10.6 lb)
Size	46.1 cm long (spacecraft radial direction) × 21.5 cm wide ×20.4 cm high
Wire Tension Limits	0.09 to 13.4 N (0.02 to 3 lb)
Operating Temperature Range	-30°C to +40°C
Radiation Exposure	100 krad

Mechanism Description

Please refer to Figure 1, Side View of the RPI Radial Antenna Deployer, Side Plate Removed, and Figure 2, Drive-End View of the RPI Radial Antenna Deployer, Electronics Cover Removed, to see a visual overview of the mechanism described in the following paragraphs in this section.

<u>Wire Storage and Transport</u>

The basic concept for wire storage is a single-layer wrap of beryllium-copper wire around a threaded aluminum spool 15.24 cm (6.000 in) in diameter. As the spool is rotated, a carrier travels along the spool tracking the threads. A pulley on the carrier guides the wire tangentially off of the spool and through a 90-degree direction change to exit the deployer parallel to the spool axis. These parts are identified in Figure 3, Detailed View of the Carrier Assembly.

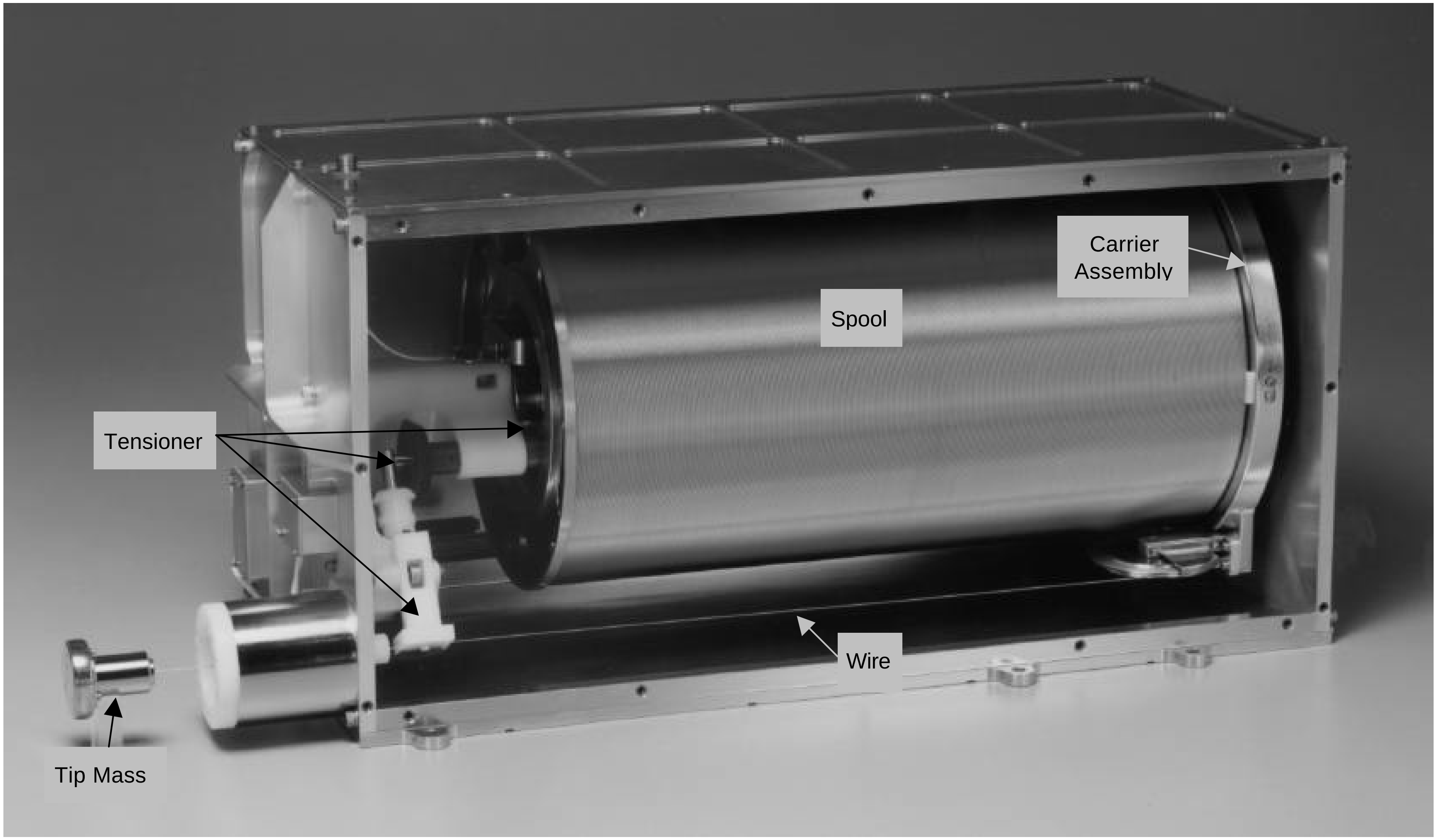

Figure 1, Side View of the RPI Radial Antenna Deployer, Side Plate Removed

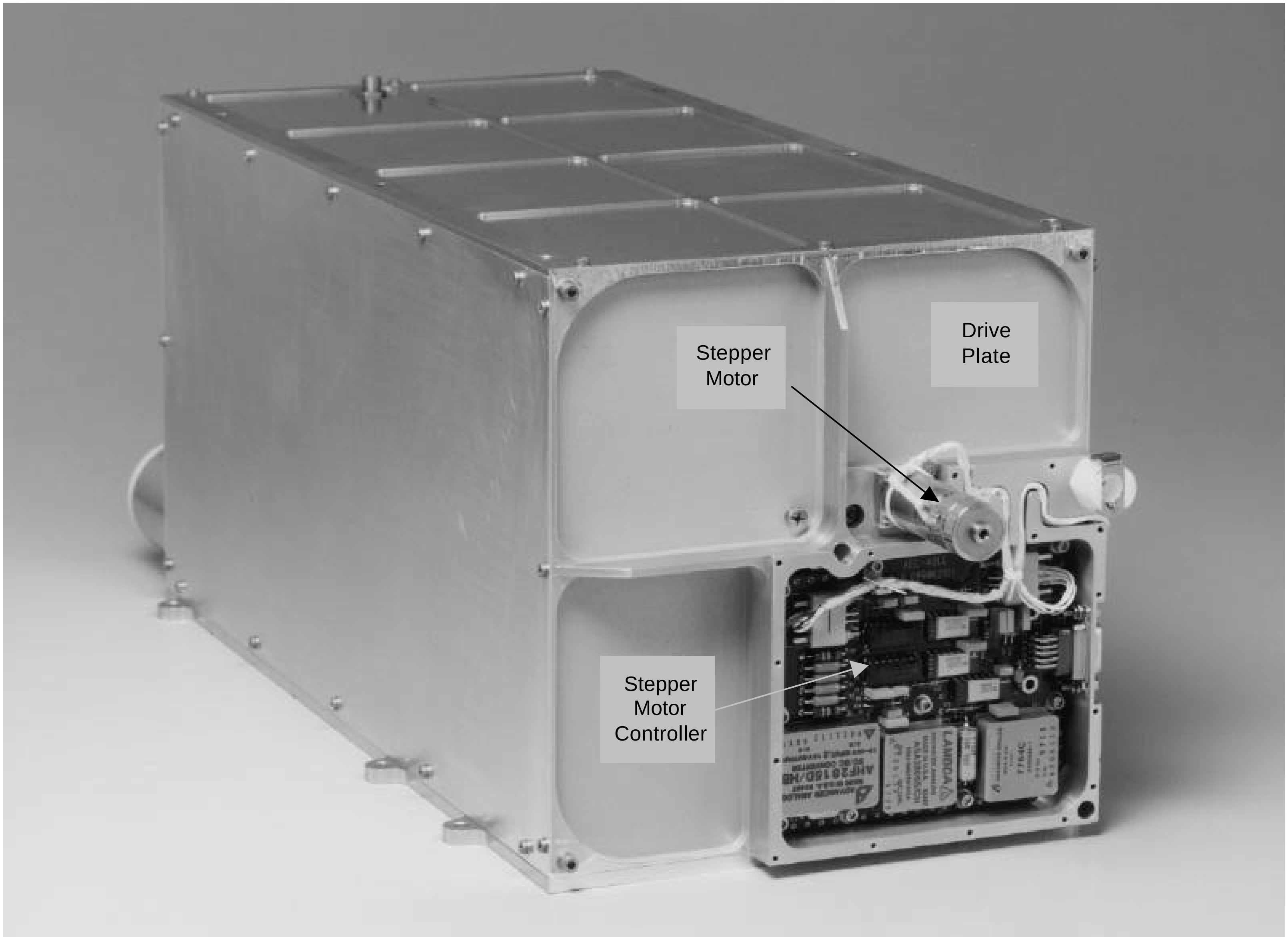

Figure 2, Drive-End View of the RPI Radial Antenna Deployer, Electronics Cover Removed

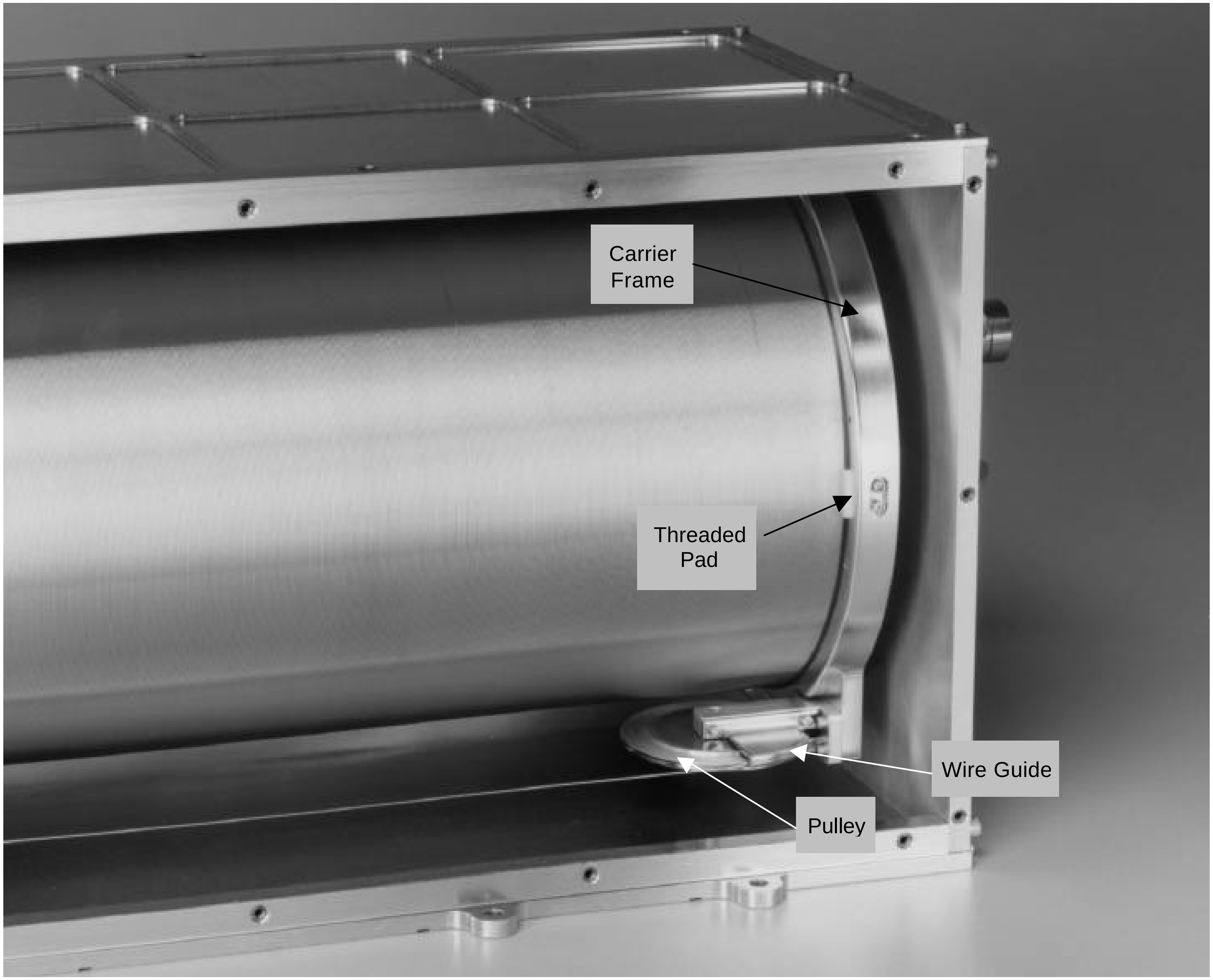

Figure 3, Detailed View of the Carrier Assembly

The carrier assembly, which engages the spool threads, consists of the following: an aluminum frame; six, threaded, Delrin pads attached around the inner diameter of the frame (one every 60 degrees) to engage the spool threads; a bracket-mounted pulley for guiding the wire on/off the spool, an anti-rotation beam to kinematically ground the carrier frame preventing its rotation about the spool axis, and counter-weights to balance the frame about the spool axis.

The diameter of the wire is the primary factor that determines the minimum thread pitch on the spool. In this case, the wire diameter is 0.4 mm (0.016 in) and the thread pitch is 48 threads per 25.4 mm. Two secondary design issues affecting the thread pitch are sufficient clearance between the mating threads of the spool and carrier to insure free rotation, and the gear ratios available on the lathe used to machine the threads. For the spool diameter used in this deployer, a diametrical clearance of 0.01 mm (0.004 in) was required between the mating threads. Since the thread height was 0.03 mm (0.012 in), this would leave nominally 0.02 mm of interference to prevent a threaded pad on the carrier from jumping a thread on the spool. Experience during vibration testing indicates that this is sufficient, but should not be reduced.

Reasons for clearances between mating threads are to accommodate imperfections in the threads on each mating part, out-of-plane free-state distortion of the carrier frame, and free-state distortions of the spool. The spools were machined from extruded tube having very little residual stress that could result in distortion during part machining, but the tooling used to support one end of the spool did create local distortions, which caused problems at final assembly.

Stepper Motor, Controller and Drive Train

In order to maintain proper stability of the spacecraft during antenna deployment, the deployment rate needed be consistent among all four deployers. A 2-phase, 6-pole stepper motor provided the best characteristics to meet the requirements for relatively slow speed and exact speed control. A magnetic detent brake integral to the stepper motor provides passive restraint of the wire deployer gear train to resist vibration and centrifugal loads encountered during launch. The magnetic detent brake was chosen instead of a more conventional power-off brake in order to minimize power consumption during motor operation.

The motor controller is integral to the antenna deployer, see Figure 4, Detailed View of the Stepper Motor Controller. It receives raw 28 V DC spacecraft power and a clock pulse from the spacecraft CPU. The controller has DC-DC converters and filters to condition the power for use by the stepper motor and control electronics. The controller also provides the connections for the limit switch harness to provide status to the CPU of deployed wire length and end-of-deployment conditions. The deployer structure surrounding the controller has a wall thickness of 46 mm to provide shielding from electron radiation; and to provide a good heat conduction path away from the controller.

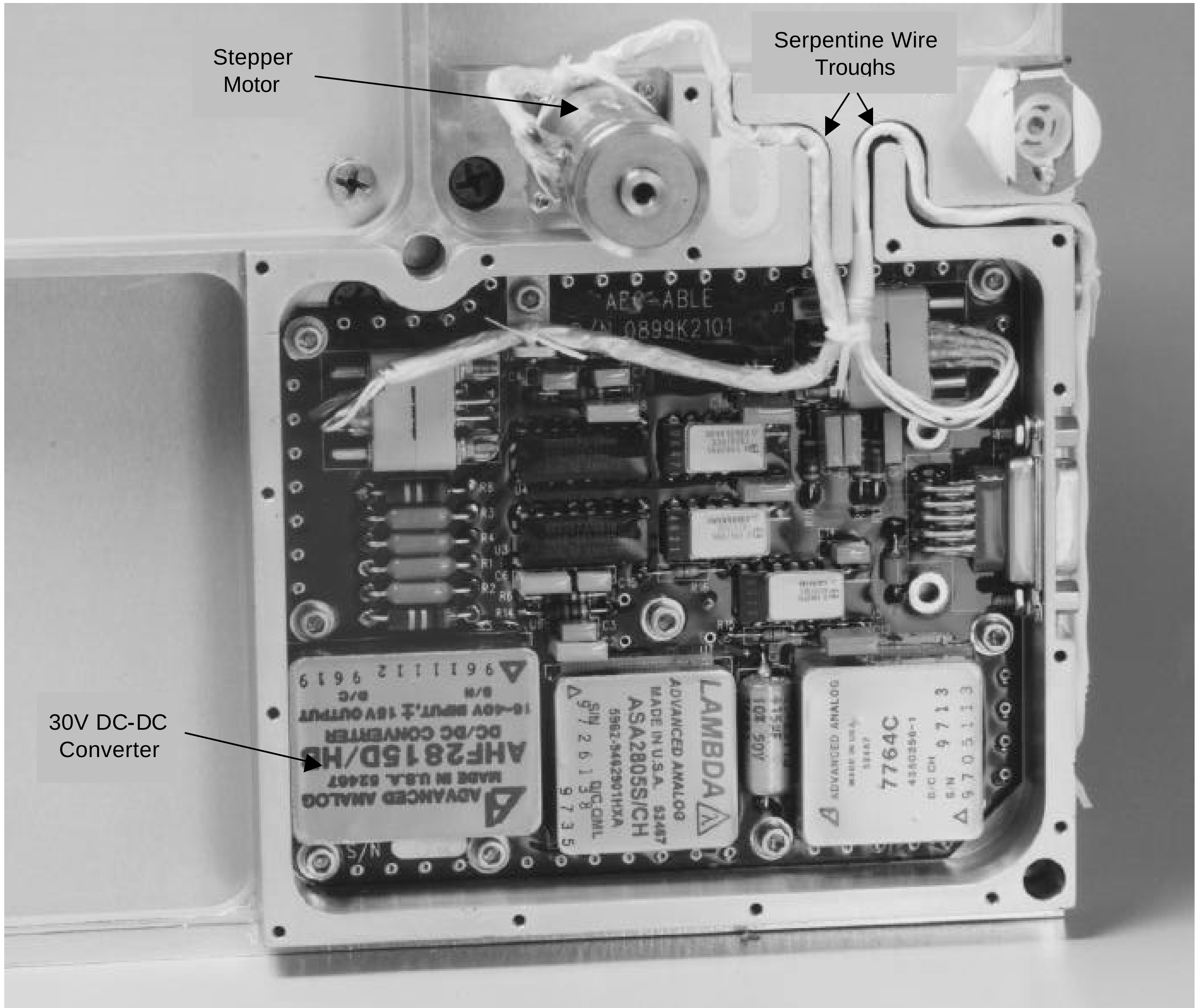

Figure 4, Detailed View of the Stepper Motor Controller

Integral to the stepper motor are two 10:1 reduction gearheads in tandem with a flat blade interface on the output shaft. The output shaft interfaces with a closed slot in one end of a Vespel SP-1 drive shaft that has a 22-tooth spur gear on the other end. This gear in-turn drives a 7075-T73 aluminum, internal, 78-tooth ring gear attached coaxially to the spool. The overall gear reduction from motor to spool is 354.6: 1. A Delrin 100AF journal supports the Vespel drive shaft and provides structural support to the spool. These material combinations resulted in low friction, low wear interfaces in the gear train and effectively insulated the stepper motor and outer deployer structure from the components experiencing high voltage. The only lubrication present is Bray 601 used in the two gearheads attached to the stepper motor. Proper design consideration had to be given to the shaft/bore clearances and gear backlash to account for the wide range of thermal expansion coefficients present in the different materials.

A significant consideration for stepper motor performance is the degradation of motor torque with winding temperature. An example of the temperature rise can be seen in Figure 5, Stepper Motor Thermal Characteristics During Vacuum Operation. The stepper motor has full current flowing through the windings at all times when energized, except during the instant that polarity is being reversed in a winding. Therefore, a significant temperature increase results as this energy is dissipated in the stepper motor. Nominally, the torque decreases linearly with the winding resistance. For copper windings the resistance increases approximately 0.4% per °C increase in temperature. In the case of the wire deployer in a +40°C thermal/vacuum environment, the steady state motor temperature averages +113°C. At this temperature, the nominal output torque at the motor gearhead is reduced to 7.5 N•m (89 oz•in) from 9.7 N•m (115 oz•in) at room temperature. This fact must be accounted for when sizing a stepper motor in order to maintain the desired torque margin. Torque margins for the four, flight wire deployers range from +2.7 to +3.5 at +40°C, except in an area of local spool distortion affecting deployment on 2 units between a narrow range of 92-95% deployed. Within that range the torque margin dips to 1.5.

<u>Deployment Wire Tensioner</u>

Due to the relatively low tension which exists in the antenna wire during some portions of deployment, a tensioning device driven by the spool rotation ensures that the antenna wire stays taught as it feeds off of the spool and around the pulley as the antenna is deployed. Please refer to Figure 6, Detailed View of the Wire Tensioner Assembly, to see the features discussed in this section. The tensioner consists of a spring-energized pawl pinching an idler roller in the pawl against the antenna wire captured in a groove of a driven-shaft. The rotation axis of the tensioner must be oriented at a right angle to the spool axis in order for the tangential motion of the grooved-shaft to be parallel to the wire motion. A coaxially mounted, internal ring gear on the exit-end of the spool drives a pinion with a bevel gear attached to the opposite end. This bevel gear drives a beveled pinion with the grooved-shaft on the opposite end that drives the wire. The bevel gears effect the right angle change of the rotating

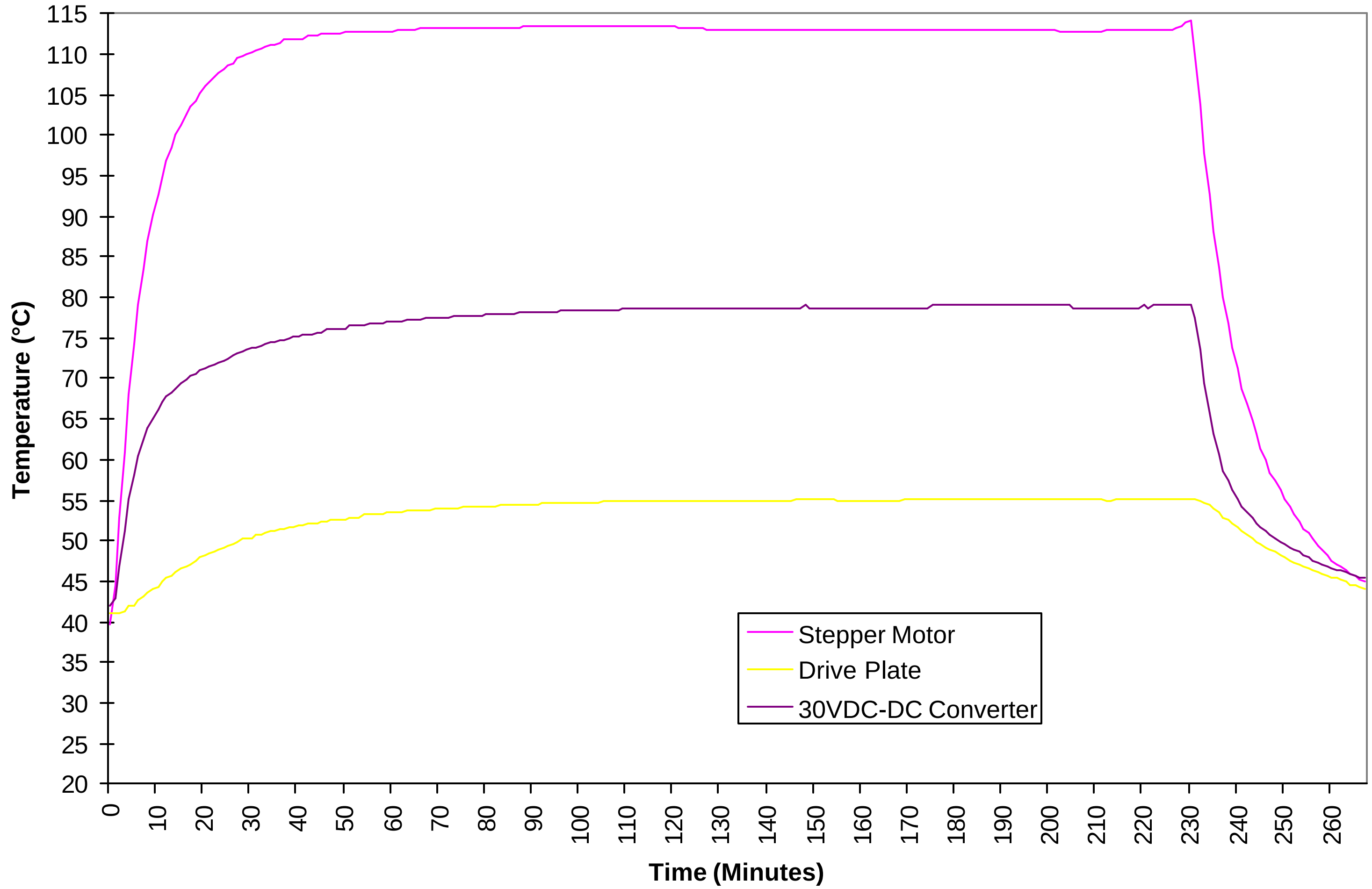

Figure 5, Stepper Motor Thermal Characteristics During Vacuum Operation

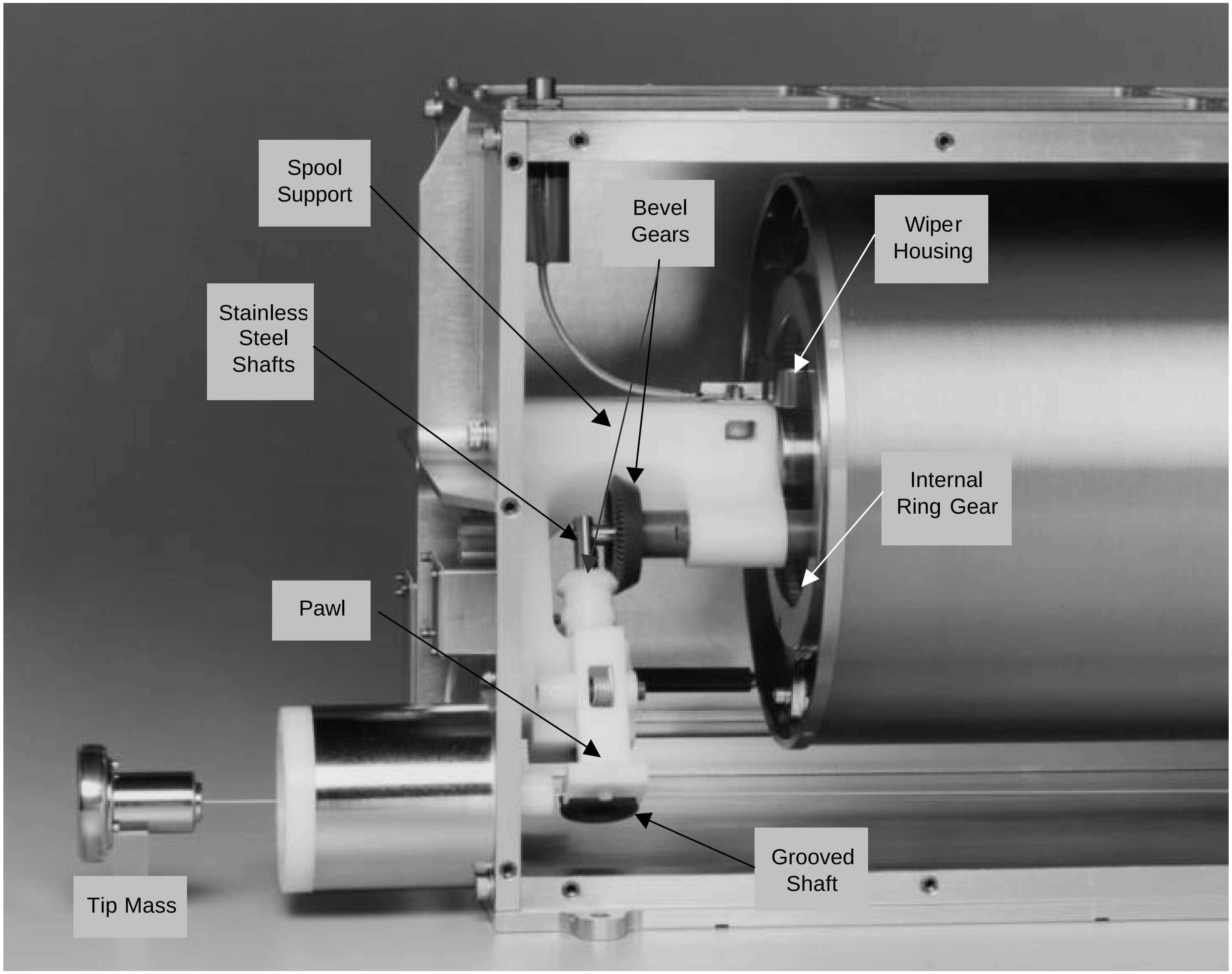

Figure 6, Detailed View of the Wire Tensioner Assembly

axis. The gear ratios of the ring gear, pinion, and bevel gears combined with the proper diameter of the grooved-shaft were sized to give a 2%-3% overdrive ratio of the grooved-shaft speed relative to the speed of the wire coming off of the spool. The pinch force and friction coefficient of the grooved-shaft were tailored to provide a tensioning force sufficient to overcome the natural tendency of the wire to straighten.

The ring gear is identical to the one on the drive-end of the spool, and drives the Delrin 100AF pinion. The bevel gear material is Delrin 100AF and drives the bevel pinion made from Delrin 100. The grooved shaft was Delrin 100AF. The pinion shaft and driven-shaft are supported by bores in the support structure for the exit-end of the spool. The spool support structure is made of Delrin 100. The alignment of the bevel gears was accomplished by two stainless steel shafts intersecting at a right angle and screwed together. A wave washer provided a preload to maintain proper mesh of the bevel gears under the specified thermal extremes. This combination of materials provides a low friction, low wear drive train with high electrical resistance and manageable thermal expansion properties.

Tip Mass/Spring Cartridge

In order to provide a higher tension in the antenna wire from centrifugal acceleration of the spinning spacecraft, a mass was attached to the end of the antenna. Instead of being merely a mass, duel functionality was added by making a spring cartridge part of the mass. This serves as a preload mechanism to take up the slack and clearances in the antenna wire and associated transport mechanisms to eliminate impact damage in the launch vibration environment.

High Voltage Conduction and Insulation

The spool is made of 6061-T6 aluminum alloy plated with an electroless nickel plating containing a co-deposite of 25% Teflon. This coating provides a conductive surface to prevent the 500+ wraps of stored wire from being a large inductor, and provides a low friction surface to minimize the drive torque required to deploy the wire. Electroless nickel plating was used on all other aluminum surfaces experiencing any wear or electrical connections in the direct path of the RPI antenna circuit. An exception to this was the internal ring gears attached to the spool, which were chemical conversion coated only.

The wipers, which conduct the signal across the rotating connection between the RPI transceiver and the antenna wire, are made from beryllium copper alloy and plated with 13 microns of hard gold. The wipers slide against the outside diameter of a protuberance from the spool hub that is plated with electroless nickel. Initially these wipers were not plated, but after a deployment cycle the resistance across the sliding interface became unstable ranging between 27 mΩ to open circuit. With the gold plating, the electrical resistance was quite consistent, typically 0.92 to 1.56 mΩ, across the following connections in series: precision ohm meter lead clip (gold on electroless nickel) to wiper housing, bolted interface between housing and wipers (electroless nickel to gold), sliding interface between wipers (2) and spool hub (gold on electroless nickel), and precision ohm meter lead clip to spool hub (gold on electroless nickel).

Electrical insulation of the high voltage components from the outer structure was accomplished by two primary means: a 1 cm (0.4 in) air gap, or 4.3 mm (0.17 in) minimum thickness of delrin. Since high voltage testing was to take place in ambient atmospheric and in vacuum environments, the air gap was sized for 5000 Volts with a generous factor of safety of four for a worst case condition of a needle point in dry air.

When using Delrin or Vespel for reliable high voltage insulators, an insulating value between 1180-1970 V/mm (30-50 V/0.001 in) should be used. This is only one tenth the short exposure dielectric strength listed in the manufacturers engineering properties for these materials. In addition, plastic insulators should not be cleaned with solvents that leave a residue or permeate the plastic. These solvent residues may break down under high voltage and create carbon arc paths.

Sharp edges approximately 0.13 mm or less in radius behave like sharp needle points, and can be sources of arcing and corona formation during exposure to high electric potential. The metallic parts were electropolished after machining to facilitate 100% burr removal and eliminate sharp “needle-point” peaks on the surface finish. Aluminum alloy 6061 was used for these parts since it could be electropolished. It is not recommended that aluminum alloy 7075 be electropolished because its magnesium content exceeds 2%. Electropolishing was an especially important process for the spools since the fine-pitch thread covers about 98% of the outside surface. Even though the thread crests were relatively sharp, this was mitigated by the close spacing of the threads and relatively shallow thread depth, and the threads did not extend to the end of the spool.

Because of the geometry of the internal ring gears and the wipers, rounding corners was either not practical (small gear teeth), or not applicable (thin metal strip). In these cases, a shield was used such that the sharp edges of these parts were surrounded by equal-potential surfaces.

Radiation Shielding

Radiation shielding does exact a weight penalty. The drive electronics had to be protected by aluminum shielding 4.6 mm (0.18 in) thick to reduce the radiation dose to 30 krad over the life of the mission. The spacecraft structure counts for an additional 0.5 mm equivalent aluminum shielding thickness. In order to minimize that impact, the stepper motor controller was made integral to the antenna deployer structure. This also enhanced the qualification and acceptance testing since a separate test sequence was not required for the drive electronics. A secondary benefit is that the additional aluminum used for radiation shielding aided conduction of heat away from the motor and controller.

Where wire harnesses penetrate the motor controller cavity, a serpentine trough was machined into the side wall for the harness to lay into. This trough needs to have geometry such that any electrons entering through the penetration must be reflected at least twice before entering the electronics cavity. This trough also serves as an excellent strain relief for the wire harnesses.

Lessons Learned

Reliable Electrical Insulators

PDR is a tough time to learn that the thickness of delrin insulators is only one-fifth what they should be for high reliability in this high voltage application. There is big difference in what value to use for dielectric strength for short duration tests versus high reliability applications. Use 1180-1970 volts per mm (30-50 volts per 0.001 in) (Ref. 1) as the dielectric strength for delrin and vespel.

Distortion of Bores in Low-Modulus Materials by Inspection Tools During Inspection

As discussed in the mechanism description, there are several instances where shafts associated with the spool or tensioner drive trains are turning in bores of Delrin parts. However, since these bores are in Delrin parts and have relatively thin wall thickness, normal inspection tooling distorted the size and/or shape of the bore to give an erroneous size measurement. A lesson learned from this is to identify bores in low-modulus materials prior to manufacturing of these parts in order to coordinate with the machinists and inspectors how the true size of the bore will be measured. This will insure the parts meet the intended design clearances.

In the case of using Deltronic pins, inspectors considered the bore to be the size of the largest diameter pin they could force through by hand. This would have resulted in much too tight of fit for what I had designed. In the case of some tensioner parts, the diameter of the 6.35 mm (0.25 in) stainless steel shafts was reduced by 0.05 mm (0.002 in) to provide the proper sliding fit necessary at the cold temperature extreme.

Another situation involved the use of a bore gauge having three radial probes that register against the bore surface when measuring the diameter. The force applied by the probes when tightened to the point at which the micrometer clutch began slipping was enough to distort a 16.88 mm (0.626 in) nominal diameter bore into a lobed shape. The actual diameter of the bore was 0.05 mm (0.002 in) smaller. Again the Vespel drive shaft was machined smaller in order to achieve the required clearance at the cold temperature extreme.

Proper Specification and Verification of Stepper Motor Performance

The stepper motor vendor selected came highly recommended. This contributed to a perception that the stepper motor procurement would be low-risk, and that some time and cost savings could result by having minimal motor testing performed by the vendor. However, when the motor began pulling out during the first functional test of the qualification unit at ambient conditions, that was our first realization that the motors did not meet the specification.

Of course much more time and cost had to be expended to correct the problem at this point than could have been potentially saved at the start of the procurement. Torque output of the original motors ranged between 44% - 72% of that required by the specification at room temperature. The major cause being that the magnetic detent brake detracted significantly from the motor torque output below 200 pps.

The solution to the problem required the following: motor winding redesign, detent torque reduction, removal of voltage dropping resistors on the motor controller in-line with the motor windings, and run-in of the motor unit with the gearhead for 3 to 5 hours in the direction of deployment at 75% of the minimum room temperature pullout torque.

These solutions were not without drawbacks. Some of the increase in torque from more current flowing through lower resistance windings was offset by an increase in the operating temperature of the motor. The margin preventing the back driving of the mechanism was reduced by the reduction of the detent force. If this problem had been discovered by the vendor during a more thorough acceptance testing, then a better solution from a technical, cost, and schedule perspective could have been realized. Namely, a 25 mm (1 in) diameter motor having a higher torque constant could have been selected which would have satisfied all of the requirements better than the solution arrived at in the eleventh hour.

Gold is Great for Sliding Electrical Contacts

Initially the wiper design did not have gold plating on the contact interface because beryllium-copper sliding on electroless nickel plating had worked well in a previous sliding application. The subtle differences between these wiper applications, and the need to have very low resistance on the order of 1 to 5 mΩ necessitated using electrolytic gold plating. In future electrical wiper applications, gold will be used to coat the copper alloy part. The cost of the gold plating is insignificant in comparison to the cost of not having it.

Importance of Mass Balance and Stiffness in Mechanisms

A significant redesign of the carrier frame on the qualification unit was needed to overcome failures of the deployer mechanism during the first attempt at passing the vibration tests. Since the carrier is able to rotate relative to the spool, any mass imbalance about this axis of rotation will impart a torque on the carrier frame when subjected to the accelerations of the vibration test. An imbalance of less than 0.045 kg (0.10 lb) resulting in a torque of 0.025 N•m (3.5 in•oz) was excited such that a bearing with a static load rating of 76 N (17 lb) that guides the end of the anti-rotation beam was brinelled. This indicates resonant frequencies in the deployer resulted in a load amplification on the order of 30 times the 14.1 G_{rms} overall random vibration loads. The 0.5 G sine sweep indicated that the response/input ratio would be at least 17:1 at 271 Hz.

Adding balancing mass to the carrier frame to eliminate over 90% of the imbalance reduced the excitation force. Stiffening the connection of the anti-torque beam to the carrier, and designing the carrier frame to engage the spool with six threaded pads instead of four reduced the dynamic amplification factor to acceptable levels.

<u>Don't Forget the Tooling!</u>

The spools were a challenging part to machine due to the tight tolerance, delicate threads machined on the outside diameter of the thin cylinder walls. The tooling to hold the spool through the various stages of machining on the lathe was critical to the success of this process. An oversight of the tooling design was to consider proper clearance of the outside diameter-to-face radius on a plug where it butted against a flange in the inside diameter of the spool. Since the plug corner radius was sharper than the fillet radius between the flange-inside diameter radius, the face of the plug could not fully seat against the flange on the spool. In addition, it was discovered later that a slight raised lip existed on the plug face due to deformation from improper handling that also contributed to the inability of the plug face to seat against the flange face. When the plug was tightened by six bolts engaging threaded holes in the spool flange, it caused distortion of the spool side walls on one end only which went undetected until the carrier was screwed on to the spool during final assembly operations. The distortion pattern coincided with the spacing of the pads on the carrier frame resulting in binding. This required repair of the spools. This problem probably existed on the qualification unit as well, but went undetected because the carrier frame with four pads was flexible enough to accommodate the six-lobe distortion pattern of the spool threads.

<u>Shipping Container Considerations</u>

The shipping environment may involve types of motions that do not exist in testing or actual launch and flight environments. Such is the case with the wire deployer. Specifically, the tumbling of a shipping container, or even resting one edge of the shipping box on the ground and allowing the other edge to drop will impart angular momentum into the spool of the wire deployer inside. When the container that has a component of rotation in its motion comes to an abrupt stop, a rather high deceleration of the deployer structure can cause a high torque to exist in the drive train between the stepper motor and the spool. This has caused the deployer antenna to lose some or all of its preload tension during shipping. Since the gear train is robust compared to the detent brake restraining torque, no damage to the gear train results, but all the same this condition is not desired. Proper consideration of these motions should be given to shipping container design of mechanisms. The shipping container should be designed to allow damped torsional compliance between the packaged deployer and the shipping container structure. The idea is to minimize rotational decelerations imparted to the mechanism by the shipping container. Figure 7, Torsionally Compliant Shipping Container Schematic contains an idea for protectively packaging a mechanism sensitive to torsional accelerations.

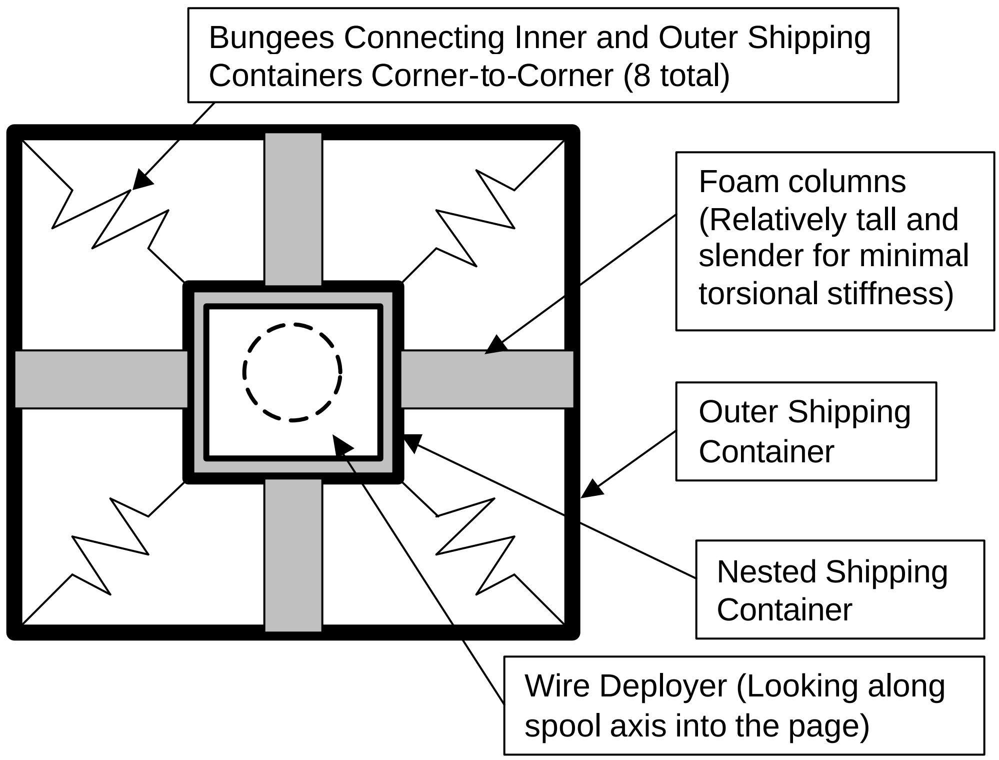

Figure 7, Torsionally Compliant Shipping Container Schematic

References

1. Battel, Steven J. Critique of RPI Wire Deployer at the Preliminary Design Review, (January 1997). Battel Engineering was acting as a consultant to Southwest Research Institute, under contract to NASA GSFC for IMAGE.